CORROSION SCIENCE AND TECHNOLOGY, Vol.31, No.2(2002), pp.122~129

# Effects of Copper and Sulfur Additions on Corrosion Resistance and Machinability of Austenitic Stainless Steel

**Soon Tae Kim, Yong Soo Park, and Hyung Joon Kim***

*Dep't of Metallurgical Engineering, Yonsei University*
*134 Shinchon-Dong, Seodaemoon-Ku, Seoul, 120-749, Korea*
*Technical Research Laboratories, Pohang Iron and Steel Co., LTD.*
*Koedong-dong, Pohang-Shi, Kyungbuk, 790-785, Korea*

Effects of Cu and S on corrosion resistance and machinability of austenitic stainless steel were investigated using immersion test, metallographic examination, Auger surface analysis and tool life test with single point turning tools. Corrosion resistance of the experimental Cu containing alloys in 18.4N $H_2SO_4$ at 80 ~ 120℃ and 3N HCl at 40℃ decreased as S content increased. However, one of the experimental alloys (Fe-18% Cr-21%Ni-3.2%Mo-1.6%W-0.2%N-3.1%Cu-0.091%S) showed general and pitting corrosion resistance equivalent to that of CW12MW in highly concentrated $SO4^{2-}$ environment. The alloy also showed pitting corrosion resistance superior to super stainless steel such as 654SMO in $Cl^-$ environment. The reasons why the increase in S content deteriorated the corrosion resistance were first, that the number and size of (Mn, Cr)S sulfides having corrosion resistance lower than that of matrix increased, leading to pitting corrosion and second, that rapid dissolution of the matrix around the pits was caused by adsorbed S. However, the alloy containing 3.1%Cu and 0.091% S maintained high general and pitting corrosion resistance due to heavily enriched noble Cu through selective dissolution of active Fe and Ni. The tool life for 3.1% Cu + 0.091% S added alloy was about four times that of 0.06%Cu + 0.005% S added alloy due to high shear strain rate generated by Cu addition giving easy cross slip of dislocation, lubrication of ductile (Mn, Cr)S sulfides adhering to tool crater surface and low cutting force resulting from thin continuous sulfides formed in chips during machining.

***Keywords*** : *austenitic stainless steel, copper, sulfur, pitting corrosion resistance, immersion test, machinability.*

## 1. Introduction

The commercial grades of AISI 304 and 316 austenitic stainless steels are so good in corrosion resistance but they are faced with many difficulties in machining compared with carbon steel and low alloy steel. The reason has been reported that work-hardening speed of machining is high and thermal conductive is low.[1] In order to improve the machinability, the material grades have been developed by adding S and Se of which AISI 303 austenitic stainless steel containing 0.15 ~ 0.3wt% S is well known and popular.[2]

However, when the sulfide inclusions are formed intentionally, which has solved Mn, Cr and Fe by adding S for the purpose of improving machinability, it comes to the problem that these inclusions will produce the pitting corrosion eventually deteriorating the corrosion resistance.[3-6] Through out the above results, it is mainly pointed out that $H_2S$ which was formed due to the solution of (Mn, Cr)S inclusions themselves is accelerating the corrosion as a roll of catalyzer. For the improvement of corrosion resistance in problem as above, it has been reported that harmful affects from S have been blocked out by adding Cu to mild steel containing S[7] while corrosion resistance has not been greatly improved by adding Cu to stainless steel containing S comparing with existing fundamental grade with no addition of Cu and S.8) So, a lot of things to be cleared up is still existing.

Meanwhile, in the critical environment of high temperature and high concentration which are highly corrosive to $H_2SO_4$ and HCl, commercial stainless steel can not be used due to poor corrosion resistance. So for such critical application, costly high super austenitic stainless steel and High Nickel base alloy are used with good corrosion resistance. Nevertheless, it is classified that those grades still belong to none-free machining material as comparing with commercial stainless steel grade, work hardening speed and toughness are very high but thermal conductivity is low which

eventually comes to the increase of production cost together with high material cost and less productivity. In this circumstance, it is significantly worthwhile in the industrial aspect if both corrosion resistance and machinability would be improved at the same time all together

On this research for the basic composition (Fe-18%Cr-21%Ni-3.2%Mo-1.6%W-0.2%N-3.2%Cu) by adding different content of S, laboratory testing has been performed for the investigation how much S will affect corrosion resistance harmfully and Cu will block out the harmful effects from S. In order to test for that, immersion corrosion behavior and Auger surface analysis have been carried out in highly concentrated 18.4N $H_2SO_4$ at 80~120℃ and in 3N HCl at 40℃. Meanwhile, for the investigation of effects of Cu and S on machinability, tool life and cutting force are measured by using the lathe attached with tool dynamometer and optical microstructure of chips is analyzed.

## 2. Experimental

The experimental alloys evaluated in this study were prepared from commercially pure grades of Fe, Ni, Fe-60.9%Mo, Fe-75%W, Fe-60.17%Cr, Fe-50%S and 57.5% Cr-35.9%Fe-6.47%N. Melting was done in a air induction furnace. After pouring the melt into ceramic mould, square type ingot (W80×L80×H320mm) and round bar type ingot ($\varphi$ 17×T7mm) ingot were manufactured. After investment casting, only solid sections of the ingots were taken to prepare test specimens. The sections were solution annealed for 70 min at 1,150℃. A small section was cut after each heat and used for chemical analysis. Table 1 shows the chemical compositions of the experimental alloys. Commercial austenitic stainless steels wroughts (AISI 316L, UR B66, 654SMO) and Ni-base alloy cast (CW12MW) as comparison materials were used.

After immersion test in 18.4N $H_2SO_4$ at 80~120℃ to evaluate general corrosion resistance and in 3N HCl at 40℃ to evaluate pitting corrosion resistance of the experimental and commercial alloys, the corrosion rates were measured by the following formula.

$$mpy = (534 \times \Delta W) \div (A \times \rho \times H) \quad (1)$$

$\Delta W$ (mg) : weight loss, A($in^2$) : surface area, $\rho$ ($g/cm^3$) : density, H(hour) : immersion time.

The number and area of inclusions were established using Image Analyzer (Model 2001, LECO Co.). The chemical composition of inclusions was established using an electron microprobe system (EPMA) equipped with both wavelength and energy dispersive spectrometer(EPMA Model 1600, Shimadzu Co.). Prior to analysis, specimens were prepared to a 1 $\mu$m diamond polish. After 1 hour immersion in 18.4N $H_2SO^4$ at 80℃, Auger surface analysis was performed on PHI 610 SAM(Scanning Auger Multi-probe, Perkin-Elmer Co.). Ar sputtering conditions were 5KeV and 500 Na. Tilt angle was 60 °.

Machinability was evaluated with a tool-life test, that is, a single point turning test and performed on a lathe which is equipped with tool dynamometer according to ISO 3685-1977(E).[9] The purposes of the test were to establish the Taylor curves Vc (cutting speed)×T (tool life) = constant for a given flank wear (0.2 mm) and cutting forces using tool dynamometer. The cutting speed was 100, 130, 160m/min, the feeding rate 0.3mm/rev., the depth of cut 1 mm and no cutting fluid was used. Flank war was measured every 30 seconds and plotted.

**Table 1. Chemical compositions of the experimental and commercial alloys**

| Alloy | Fe | C | Si | Mn | Ni | Cr | Mo | W | N |
|---|---|---|---|---|---|---|---|---|---|
| Base* | Bal. | 0.036 | 0.85 | 1.44 | 21.2 | 18.3 | 3.23 | 1.64 | 0.23 |
| 3Cu* | Bal. | 0.034 | 0.98 | 1.50 | 21.1 | 18.2 | 3.21 | 1.61 | 0.21 |
| 3Cu4S* | Bal. | 0.033 | 1.19 | 1.50 | 21.6 | 18.6 | 3.11 | 1.65 | 0.22 |
| 3Cu9S* | Bal. | 0.034 | 1.05 | 1.59 | 21.2 | 18.1 | 3.03 | 1.63 | 0.23 |
| B* | Bal. | 0.033 | 0.81 | 1.52 | 20.8 | 22.3 | 6.2 | - | 0.24 |
| C* | Bal. | 0.032 | 0.84 | 1.48 | 21.6 | 23.8 | 6.63 | - | 0.32 |
| AISI 316L** | | Bal. | 0.02 | 0.35 | 1.21 | 14.1 | 17.2 | 2.6 | - |
| UR B66** | Bal. | 0.02 | 0.32 | 1.23 | 22.0 | 24.0 | 6.0 | 2.0 | 0.4 |
| 654SMO** | Bal. | 0.02 | 0.36 | 1.31 | 22.0 | 24.0 | 7.3 | - | 0.5 |
| CW12MW** | | 7.61 | 0.061 | 0.93 | 1.46 | Bal. | 14.4 | 16.7 | 4.83 |

* : experimental alloy(cast), ** : commercial alloy(wrought)

## 3. Results and discussion

### 3.1 Effects of microstructures on immersion corrosion behavior

Figure 1 shows the number and area of (Mn, Cr)S type inclusions in the experimental alloys solution annealed for 150 min at 1,150℃. As S content in the experimental alloys containing Cu is increased, the number and area of inclusions is increased and the average length of inclusions is increased from 3.4 $\mu$m to 4.3 $\mu$m. Figure 2 shows the effect of Cu and S content on corrosion rate of the experimental alloys and commercial alloy (CW 12 MW) in 18.4N H2SO4 at elevated temperatures. As S content in Cu added experimental alloys and temperature of $H_2SO_4$ solution is increased, corrosion rate is increased. However, corrosion resistance of the experimental alloy 3Cu9S containing 0.091S is equivalent to that of the most expensive Ni-base alloy (CW12MW). Figure 3 shows optical micrographs of the experimental alloys after a 24-hour immersion in 18.4N $H_2SO_4$ at 80℃. The experimental alloy not containing Cu was severely corroded. However, as S content in the experimental alloys containing Cu is increased, pitting corrosion is produced at (Mn, Cr)S inclusions less corrosion resistant than matrix. Corrosion resistance of the experimental alloys containing Cu regardless of added S content is superior to that of the more expensive 654SMO super austenitic stainless steel in highly concentrated $SO4^{2-}$ environment.(Table 2)

**Table 2. Corrosion rate of the experimental and commercial alloys in 18.4N $H_2SO_4$ at elevated temperatures and in 3N HCl at 40℃.**

| Alloy | 18.4N $H_2SO_4$ | | | | | 3N HCl |
|---|---|---|---|---|---|---|
| | 80℃ | 90℃ | 100℃ | 110℃ | 120℃ | 40℃ |
| Base | 7,907 | 12,507 | 17,572 | 22,482 | 27,694 | 87.2 |
| 3Cu | 7.9 | 14.0 | 23.0 | 38.7 | 61.1 | 18.9 |
| 3Cu4S | 11.0 | 17.3 | 29.0 | 49.7 | 85.5 | 20.7 |
| 3Cu9S | 11.8 | 18.2 | 32.1 | 50.5 | 102 | 23.2 |
| B | 4,957 | - | - | - | - | 59.4 |
| C | 851 | - | - | - | - | 57.1 |
| AISI 316L | 34,680 | - | - | - | - | 387.8 |
| UR B66 | 21.9 | 61.4 | 286 | 1,679 | 1,924 | 39.9 |
| 654SMO | 121 | 178 | 811 | 2,086 | 3,303 | 32.6 |
| CW12MW | 10.2 | 19.3 | 34.2 | 51.5 | 98.5 | 19.7 |

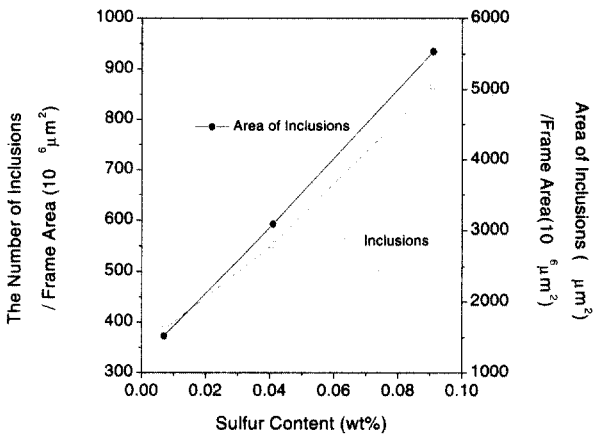


**Fig. 1.** Effect of sulfur content on the number corrosion rate of the experimental alloys experimental alloys containing copper.

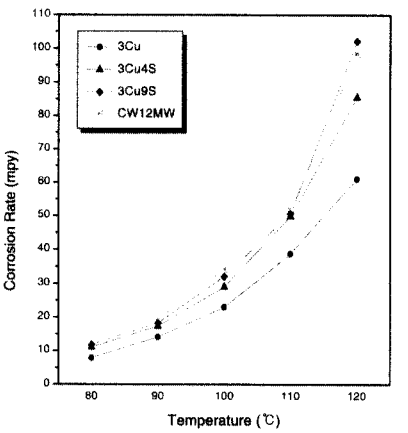


**Fig. 2.** Effect of copper and sulfur content corrosion rate of the experimental alloys and the commercial alloy (CW12MW) in 18.4N $H_2SO_4$ at elevated temperatures.

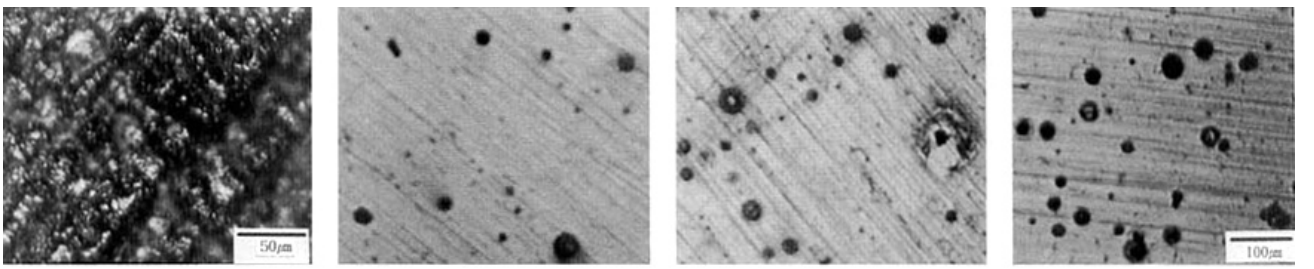


(A) (B) (C) (D)

**Fig. 3.** Optical micrographs of the experimental alloys after a 24-hour immersion in 18.4N $H_2SO_4$ at 80℃.
(A) Base(0.06%Cu+0.005%S) (B) 3Cu(3.2%Cu+0.007%S) (C) 3Cu4S(3.2%Cu+0.041%S) (D) 3Cu9S(3.1%Cu+0.091%S)

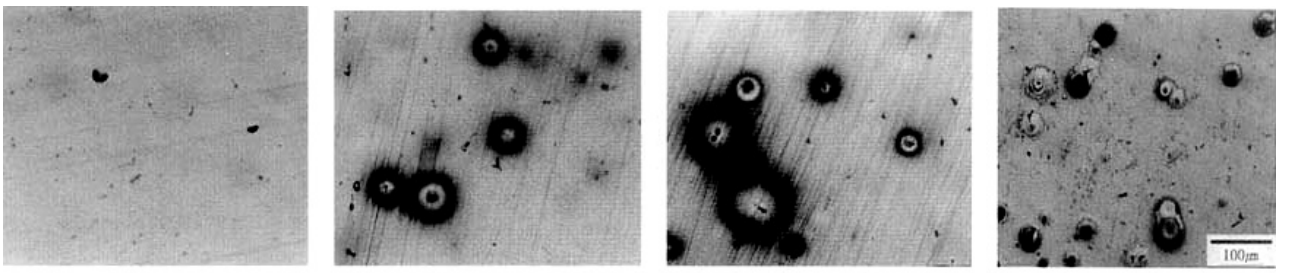


(A) (B) (C) (D)

**Fig. 4.** Optical micographs of the corrosion progression of the experimental alloy 3Cu9S in 18.4N $H_2SO_4$ at 80℃. (A) As polished (B) 15min-immmersion (C) 1 hour-immersion (D) 6 hour-immersion

Therefore, corrosion resistance of the experimental alloys containing Cu depends on the number and area of (Mn, Cr)S inclusions. Comparing corrosion rate (102mpy) of the experimental alloy containing 3.1%Cu + 0.091%S with corrosion rate (61.1mpy) of the experimental alloy containing 3.2%Cu + 0.007%S in 18.4N $H_2SO_4$ at 120℃, general corrosion about the degree of 60% is produced at matrix and pitting and general corrosion about the degree of 40% is produced at (Mn, Cr)S inclusions and S adsorbed matrix around the pits. Table 2 also shows that pitting corrosion resistance of the experimental alloy containing 3.2%Cu is superior to that of Base, B, C and commercial super austenitic stainless steel such as 654SMO in 3N HCl at 40℃.

Effects of Cu and S Additions on General and Pitting Corrosion Resistance

Figure 4 shows optical micrographs of the corrosion progression of the experimental alloys 3Cu9S in 18.4N $H_2SO_4$ at 80℃. At the initial step of corrosion (Figure 9, (B)), pitting corrosion is produced at (Mn, Cr)S inclusions having corrosion resistance lower than that of matrix. As immersion time increases (Figure 9, (C), (D)), the sulfides were perfectly corroded and the matrix adsorbed S around the pits was severely dissolved. It had been reported that rapid dissolution of the matrix around the pits was caused by S adsorption. The S rings have its origin the decomposition of thiosulfate ($S_2O_3^{2-}$) produced by the anodic dissolution of the inclusions.[10-12] The evidence supports models of the initiation of pitting corrosion which attribute the effect of sulfide inclusions on the acceleration of anodic dissolution kinetics caused by adsorbed sulfur. The oxidation of $S_2O_3^{2-}$ into adsorbed S can be expressed as follows.

$$2MnS + 3H_2O = 2Mn^{2+} + S_2O_3^{2-} + 6H^+ + 8e^- \quad (2)$$

$$S_2O_3^{2-} + H_2O = S + SO_4^{2-} + 2H^+ + 2e- \quad (3)$$

Another possible reaction is as followsp[12]

$$3MnS + 6H^+ = 3Mn^{2+} + 3S + 3H_2 \quad (4)$$

Meanwhile, as another report, when sulfides are dissolved in acid solution, $H_2S$ is produced.[13]

$$MnS + 2H^+ = H_2S + Mn^{2+} \quad (5)$$

According to the above reaction, $H_2S$ in aerated acid solution is chemically adsorbed on surface and increases catalytically the anodic dissolution and hydrogen evolution rate. The above results was focused on the decrease of corrosion resistance by (Mn, Cr)S inclusions, S adsorbed around the pits and the increase of anodic dissolution and hydrogen evolution rate by catalytic $H_2S$.

However, in this study we focused on the reason why the experimental Cu containing alloys maintained high corrosion resistance despite the addition of S. Figure 5 shows Auger surface analysis of the experimental alloys after 1 hour immersion in 18.4N $H_2SO_4$ at 80℃.The surface composition of matrix around pits of the experimental alloy containing 3.1%Cu + 0.091%S is similar to that within the pits. It was suggested as the primary reason of this result that the protective surface film on the alloy containing 3.1%Cu + 0.091%S was heavily enriched by the noble metallic Cu and CuO from the selective dissolution of the active metallic Fe, Ni and the active FeS, NiS, $FeSO_4$, $NiSO_4$ produced by S adsorption. But the 3.2% Cu added experimental alloy containing a little S shows a little Cu enrichment because of a little dissolution of the active Fe and Ni by a little S adsorption. From this result the corrosion resistance of the alloy was maintained by Cu and Ni.

### 3.2 Effects of cutting speed and Mn/S ratio on tool life

Tool life is affected most heavily by cutting speed. The related formula between cutting speed and tool life, devised by Taylor, is as follows.[14]

$$VT^n = C \quad (6)$$

(V : cutting speed (m/min), T : tool life (min), C, n : constant)

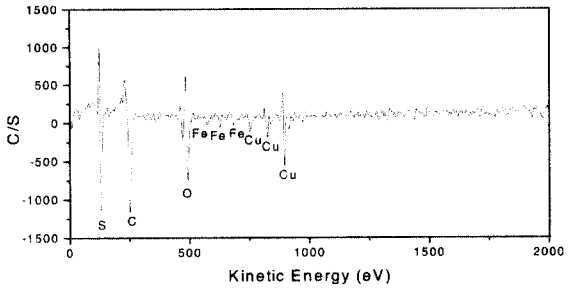


(A) 3Cu9S(Within the pit)

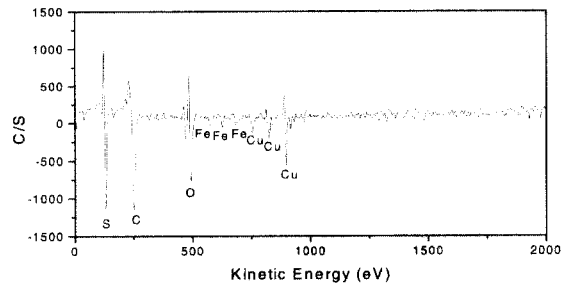


(B) 3Cu9S(Around the pit)

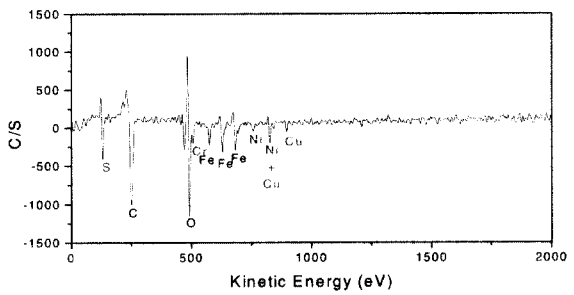


(C) 3Cu(Matrix)

**Fig. 5.** Auger surface analysis of the experimental alloys after 1hour immersion in 18.4N $H_2SO_4$ at 80℃

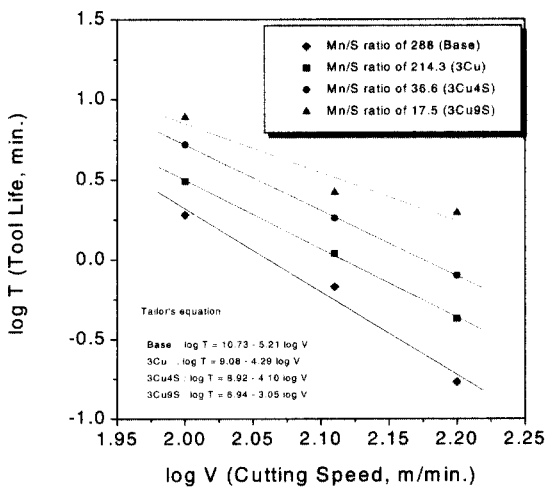


**Fig. 6.** Effect of cutting speed on the tool life performance of the experimental alloys.

Figure 6 shows effect of cutting speed on the tool life performance of the experimental alloys. When it comes to flank wear of VB = 0.2 mm, the more decreased Mn/S ratio and cutting speed are, the more increased tool life is. In case that cutting speed is 100m/min, the experimental alloy containing 3.2% Cu has been improved by 1.6 times in tool life comparing with the alloy not containing Cu while the experimental alloy containing 3.1% Cu+0.091%S has been improved by 4 times in tool life. This improvement of tool life is considered due to the synergistic effect on Cu+S.

### 3.3 Belag observation on wear surface of tool crater

(A) and (B) of Figure 7 are the SEM micrographs and chemical composition of crater wear after machinability. As the more decreased Mn/S is, the more decreased crater wear is, tool life is increased. (C) and (D) of Figure 15 indicate the analyzed results of EDS composition for the crater wear surface of the experimental alloys. When Mn/S ratio is decreased, firstly, Mn and S of matrix are increasing Cr, Ni and Fe are decreasing. This means it is understood that tool crater wear is obviously decreased as softened (Mn, Cr) S sulfides in machining will form the Belag on the crater surface, i.e. lubricating film[15] which is protecting direct attack from chips and sheared plane into the crater surface and control the workability of tool against chips secondly, tungsten carbide tool to be used when machining as a matrix of WC+Co is coated by 3 layers in the sequence of TiCN, $Al_2O_3$ and TiN from tool surface to bulk. When Mn/S ratio is decreased, Al content is increased but Ti is decreased due to the formation lubricating film. It is considered that wear on coated layers is decreased comparing with the experimental alloy which has big share of Mn/S ratio.

### 3.4 Mechanism of machinability improvement by Cu and S additions

Figure 8 shows effect of Mn/S ratio on cutting force for the experimental alloys. It is considered that tool life is improving as the more decreased Mn/S ratio is, the more decreased the cutting force affecting the rake surface of tool is. Figure 9 shows effect of Mn/S ratio on shear strain rate of the experimental alloy, which is available by following formula.[16]

$$\gamma = v \cos \alpha \div d \cos(\varphi - \alpha) \quad (7)$$

($\gamma$ : shear strain rate, v : cutting speed, $\alpha$ : rake angle, d : widths of work-hardened zone)

The width of work-hardened zone is measured as 0.062mm in case of Base tested alloy, 0.026mm : 3Cu tested alloy alloy, 0.026mm : 3Cu4S tested alloy and 0.024

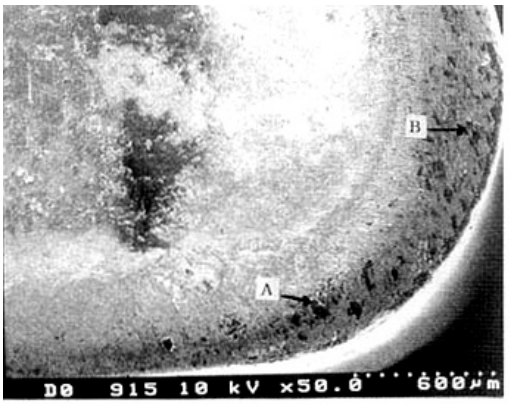


(A) Base experimental alloy

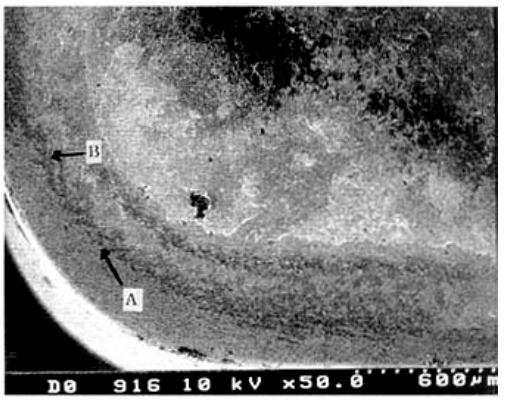


(B) 3Cu9S experimental alloy

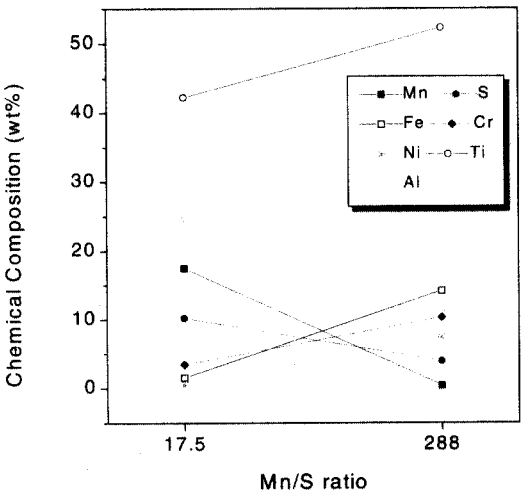


(C) Chemical composition at point A

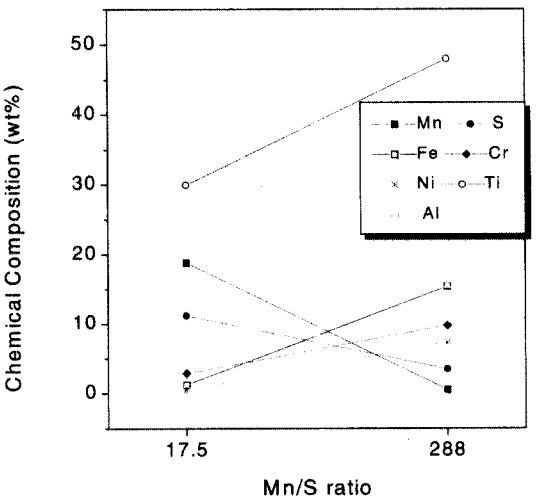


(D) Chemical composition at point B

**Fig. 7.** SEM micrographs and chemical composition of crater wear surface after machinability. (cutting speed:100 m/min, feeding rate:0.3mm/rev., cutting depth:1mm and no cutting fluid)

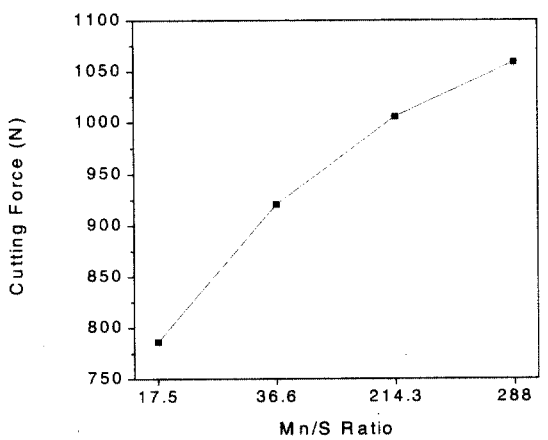


**Fig. 8.** Effect of Mn/S ratio on cutting force of the experimental alloyw.(cutting speed:50m/min, feeding rate:0.3mm/rev., cutting depth:1mm and no cutting fluid)

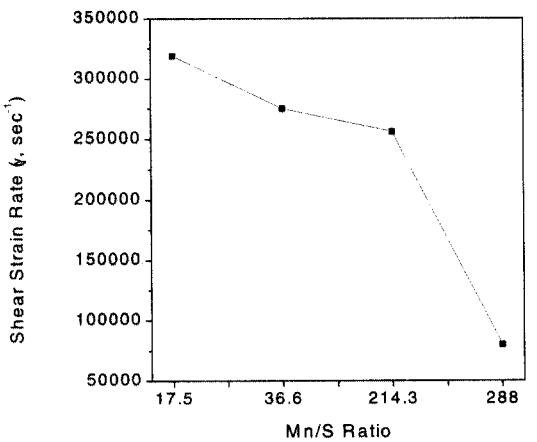


**Fig. 9.** Effect of Mn/S ratio on shear strain rate of the experimental alloyw.(cutting speed:100m/min, feeding rate:0.3mm/rev., cutting depth:1mm and no cutting fluid)

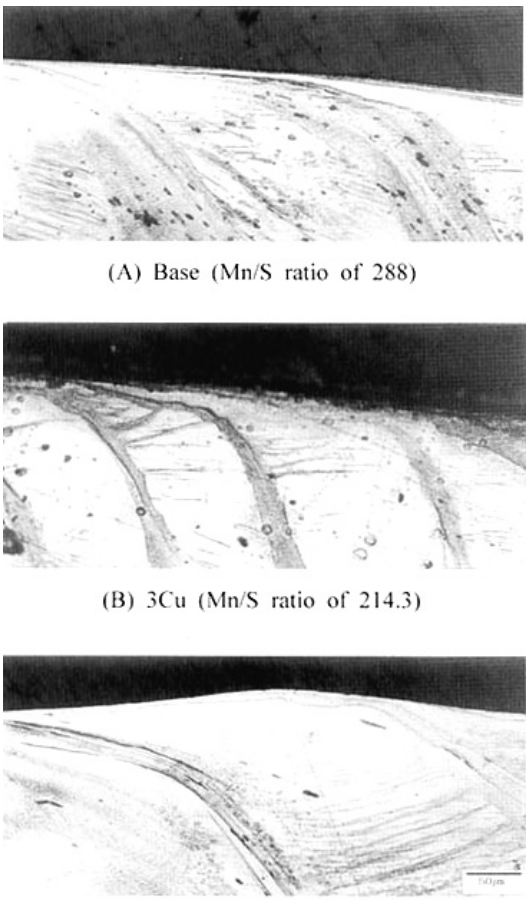

(A) Base (Mn/S ratio of 288)

(B) 3Cu (Mn/S ratio of 214.3)

(C) 3Cu9S (Mn/S ratio of 17.5)

**Fig. 10.** Cross section of machined chips showing the effect of Mn/S ratio and Cu addition on the primary and secondary shear zone. (cutting speed:100 m/min, feeding rate : 0.3mm/rev., cutting depth:1mm and no cutting fluid)

mm : 3Cu9S tested alloy respectively. There, it is getting appeared that the more decreased Mn/S ratio, the more increased shear strain rate. Meanwhile, Figure 10 shows effect of Mn/S ratio and Cu addition on optical microstructures of machined chips of the shear zone. As the width of work-hardened zone is widely formed at primary and secondary shear zone of Base tested alloy which has high Mn/S ratio and containing 0.06%Cu+ 0.005%S, shear deformation is not easily appeared. Meanwhile, tested alloy 3Cu which has smaller Mn/S ratio than tested alloy Base and containing 3.2%Cu+0.007%S is showing that the narrow widths of work-hardened zone are formed at the primary and secondary shear zone. This means that shear deformation easily appeared. The reason is that Cu adding for the experimental alloy is one of the well-known elements[17] increasing SFE(Stacking Fault Energy). By adding 3.2% Cu, SFE is increased combining two partial dislocations with one perfect dislocation and giving easy cross slips into the neighbor slip plane which eventually come to less work-hardening and easy shear deformation. Tested alloy (3Cu9S) which less Mn/S ratio, to be added by high S (0.091%) and containing 3.1% Cu is making very easy shear deformation due to the addition of Cu increasing SFE. Furthermore, when machining, as ductile sulfides are deformed in narrow and tangential cutting force, i.e., shear stress is decreased and normal cutting force at rake face of tool is also decreased which are having improvement of tool life . Another roll of sulfides as mentioned is to provide lubrications adhering crater surface of tool which eventually comes to decreasing the tool wear.

## 4. Conclusions

1) Corrosion resistance of the experimental Cu containing alloys in 18.4N $H_2SO_4$ at 80 ~ 120℃ and 3N HCl at 40℃ decreased as S content increased. However, one of the experimental alloys (Fe-18%Cr-21%Ni- 3.2% Mo-1.6%W-0.2%N-3.1%Cu-0.091%S)showed general and pitting corrosion resistance equivalent to that of CW12MW in highly concentrated $SO4^{2-}$ environment. The alloy also showed pitting corrosion resistance superior to super stainless steel such as 654SMO in $Cl^-$ environment.

2) The reasons why the increase in S content deteriorated the corrosion resistance were first, that the number and size of (Mn, Cr)S sulfides having corrosion resistance lower than that of matrix increased, leading to pitting corrosion and second, that rapid dissolution of the matrix around the pits was caused by adsorbed S. However, the alloy containing 3.1%Cu and 0.091% S maintained high general and pitting corrosion resistance due to heavily enriched noble Cu through selective dissolution of active Fe and Ni.

3) The tool life for 3.1% Cu + 0.091% S added alloy was about four times that of 0.06%Cu + 0.005% S added alloy due to high shear strain rate generated by Cu addition giving easy cross slip of dislocation, lubrication of ductile (Mn, Cr)S sulfides adhering to tool crater surface and low cutting force resulting from thin continuous sulfides formed in chips during machining.

## References

1. S. Gunnarsson, *Stainless Steel* '92, **1**, 149, (1992).
2. T. Nakamura, *97 kai Nishiyama Kinenkosa*, Nihon Tetskogyokai, 201 (1984)
3. B. E. Wilde and J. S. Armijo, *Corrosion*, **23**, 203 (1967).
4. G. Wranglen, *Corros. Sci.*, **14**, 331 (1974)
5. G. Karlberg, *Scand. J. Met.*, **3**, 46 (1974)
6. K. Takaizawa, Y. Shimizu, E. Yoneda, H. Shoji and I.

Tamura, *Proceedings of 10th World Congress on Metal Finishing*, p.453 (1980).
7. H. J. Cleary and N. D. Greene, *Corros. Sci.*, **7**, 821 (1967).
8. K. Ono, Tets-to-go, S811 (1977).
9. Technical Committee ISO/TC 29, *Tool-life Testing with Single-point Turning Tools*, ISO 3685-1977 (E).
10. Anthony R. J. Kucernak, Robert Peat and David E. Williams, *J. Electrochem. Soc.*, **139**, 2337 (1992).
11. J.E. Castle and Ruoru Ke, *Corros. Sci.* **30**, 409 (1990).
12. R. C. Alkire and S. E. Lott, *J. Electrochem. Soc.*, **136**, 973 and 3256 (1989).
13. P. Sury, *Corros. Sci.*, **16**, 879(1976).
14. F. W. Taylor, *Trans. A.S.M.E.*, **28**, 31 (1907).
15. C.W. Kovach, Proceeding International Symposium on Sulfide Inclusions in Steel, *ASM, Port Chester*, p. 459, (1974).
16. P. B. Oxley and M. G. Stevenson, *J. Inst. Met.*, **95**, 308 (1967).
17. D. Delieu and J. Nutting, *Iron Steel Inst.*, London, Spec. Rept. **86**, 140(1964).